ARTICLE

Dynamics within Alkylsiloxane Self-Assembled Monolayers Studied by Sensitive Dielectric Spectroscopy

Mary C. Scott, Derrick R. Stevens, Jason R. Bochinski, and Laura I. Clarke*

Department of Physics, NC State University, 2401 Stinson Drive, Box 8202, Raleigh, North Carolina 27695

ABSTRACT Self-assembled monolayers are a ubiquitous laboratory tool and have been the subject of many experimental investigations which have primarily focused on static properties of full coverage monolayers, with the maximum density and ordering possible. In this work, dynamics within low density, planar siloxane self-assembled monolayers are studied utilizing highly sensitive dielectric spectroscopy. Dilute, disordered films were intentionally fabricated in order to study the widest range of possible motions. At low coverage, an interacting relaxation is observed, which has similar dynamics to polyethylene-like glass transitions observed in phase-segregated side-chain polymers, despite the rigidity of the substrate and the constraint of ethyl groups in relatively short chains. As density is increased, a second local relaxation, previously observed in three-dimensional SAMs and associated with rotation within a small segment of the alkyl chain, is also observed.

KEYWORDS: monolayer · rotational dynamics · siloxane · dielectric spectroscopy

Self-assembled monolayers (SAMs) are well-established systems for scientific and technological investigations due to their ease of preparation, physical robustness, and facile ability to controllably modify chemical properties of surfaces. A brief sampling of the diverse applications for which SAMs have been utilized include creation of new molecular devices,[1] lithographic patterning,[2,3] reduction of friction, alteration of surface wetting (*i.e.*, hydrophobic *versus* hydrophilic), corrosion protection, light-activated switching,[4] and acting as an interfacial layer in biological applications[5] as well as stationary phases for shape recognition in liquid chromatography.[6−8] SAMs are also utilized in surface modification of metal nanoparticles, enhancing the particles' solubility and preventing aggregation into larger metal clusters.[9,10] Nanoparticle−monolayer systems are referred to as 3D SAMs and have been used in previous studies of molecular dynamics within monolayers as the increased surface area provides higher signal size, although structural and dynamic properties may differ from planar 2D SAMs, where molecular attachment occurs onto flat surfaces. Dynamics within planar SAMs are the focus in this report.

The two most commonly utilized covalently bound SAMs are those created by utilizing thiol-based or silane-based chemistry, with the sulfur (silicon) headgroup forming the chemical linkage to the appropriate metallized (hydroxylated) surface, an alkyl carbon chain with varying available lengths, and an application-specific, functionalized chemical group at the end of the chain. Siloxane monolayers may be fabricated with or without cross-linking; furthermore, they generally exhibit a lower level of order than their thiol counterparts. Extensive previously published work on high density alkylsiloxane and alkanethiol films indicates that the film ordering increases with chain length due to enhanced intermolecular interactions. These interactions can also lead to growth *via* island formation (particularly from solution phase). When shorter length chains (<5 carbon chain length) are used, or at dilute coverage, a more disordered film results; disordered monolayers are often described as "liquid-like" in contrast with the more ordered "solid-like" structures. Deposition temperature and technique also affect film order with lower temperature, solution phase samples typically the most ordered, and high temperature, vapor-phase depositions significantly more disordered.

Research on SAMs has usually focused on mechanisms of growth and procedures for optimization, having the implied goal to generate full coverage, monolayer films, with alkanethiols on Au(111) regarded as the archetype of an ordered (near crystalline) 2D SAM.[11,12] In contrast, in this report, we study dynamics within monolayers with varying intermolecular interactions (due either to molecular structure or density), de-

*Address correspondence to laura_clarke@ncsu.edu.

Received for review August 31, 2008 and accepted October 18, 2008.

Published online November 7, 2008.
10.1021/nn800543j CCC: $40.75

gree of ordering, and molecular structure. Within our approach, the purpose of the planar surface is to act as a means to physically constrain the collection of molecules under study, so that the attachment point of each molecule cannot move, and the overall molecular density is experimentally fixed, while retaining significant conformational freedom (particularly at low densities). This experimental design, combined with the highly sensitive technique employed, enables observation of the interplay of intramolecular, intermolecular, and molecule−substrate interactions in determining resultant molecular dynamics. Such basic understanding of the possible motions of molecular assemblies on surfaces remains an important area of nanoscale scientific focus, both for development of new technologies[13] and for further expanding fundamental knowledge, which connects the morphological structure and motional behavior of the bound molecules on the microscopic level to the overall physical properties of the resultant film at the macroscopic scale. Furthermore, these experiments enable future manipulation of molecular dynamics, for instance, by introduction of strong molecule−molecule interactions that could result in previously unexplored phase transitions within this quasi-two-dimensional environment.

In this work, we utilize alkyl-terminated monolayers in order to connect with previous dynamics studies of alkanes, including plastic crystal phases within solid alkanes,[14] relaxations within polymers with an alkane backbone,[15,16] and the dynamics of phase-separated, alkyl side chain containing polymers.[17] Thus, the presence, absence, modification, or creation of new or previously observed dielectric relaxations within a SAM reveals how the local environment, including restriction of the molecular center-of-mass and arrangement on a planar surface, influences the motional possibilities of this most basic hydrocarbon structure. We make use of silane chemistry, as siloxane monolayers may be fabricated with or without cross-linking, providing increased flexibility to create variation in film structure and chain-to-chain interactions. Vapor-phase depositions at high temperature are utilized as a solvent-free mechanism to produce dilute, homogeneous films without island formation. Beginning with these dilute, disordered structures, the transition to a dense, more ordered monolayer, and the associated changes in dynamics, can be systematically observed. In particular, we observe an interacting relaxation in alkylsiloxane monolayers with varying chain length from 4 to 18 carbons and densities varying from 10% to multilayer coverage. The relaxation occurs in the same location and disperses with frequency in a similar manner to polyethylene-like glass transitions observed in polymers with phase-segregated alkyl side chains. At higher density, a localized relaxation, which has Arrhenius dynamics, is observed, consistent with a previous report utilizing a 3D approach,[18] and assigned to a similar local motion within polyethylene (PE).

Myriad characterization techniques have been applied to SAMs,[11] such as scanning tunneling microscopy (STM), atomic force microscopy (AFM), nuclear magnetic resonance (NMR), neutron scattering, infrared spectroscopy, differential scanning calorimetry (DSC), as well as various forms of electron and X-ray spectroscopy. One challenge in studying 2D SAMs is the intrinsically small signal size due to the implicit monolayer nature of the system, thus few standard characterization techniques are sufficiently sensitive, and alternative approaches must be developed.[10] In particular, techniques such as NMR, DSC, and transmission infrared spectroscopy have usually only been applied to 3D SAMs with subsequent enhanced signal size. Furthermore, while molecular scale samples can be observed with scanning probe techniques, these techniques provide primarily quasi-static data. Thus it is highly technically challenging to observe *dynamical* processes within 2D SAMs.

In the present work, we employ a low frequency dielectric relaxation spectroscopy approach to observe molecular motion within well-characterized self-assemblies of surface-bound molecules attached to planar nonconducting substrates. By utilizing substituted alkyls to create a dipole moment or the small induced dipoles near the siloxane terminus, the alkyl chains are rendered dielectrically active. Dielectric spectroscopy measures the ability of dipolar objects within a sample to reorient in response to an applied electric field, by creating an observable electrical polarization, as a function of field frequency and sample temperature. In the most common "broadband" approach, a sample is placed between two macroscopic metal plate electrodes and subjected to a wide range of frequencies (from 10^{-5} to 10^{7} Hz) at a single, fixed temperature, typically near ambient. The technique utilized in this work differs from this method in two important ways. First, in order to increase sensitivity, a relatively narrow band of frequencies, centered about 1 kHz, is primarily used, wherein low-loss fused silica reference capacitors are available. Second, as a replacement for the macroscopic dual electrode configuration, basic lithographic patterning is used to create an array of interdigitated planar electrodes, restricted to a single flat substrate. The subsequent 2D SAMs are grown on the insulating surface in the regions between the metal electrodes. This technique is particularly appropriate for these ultrathin film measurements as the relative height of the electrodes *versus* the thickness of the monolayer results in a near-parallel electric field at the substrate surface. In addition, the fringing electric field penetrates into the spatial regions above and below the electrode plane. We note that this experimental technique could be usefully applied to dynamical measurements of free-standing, thin polymer films, wherein confinement and

surface induced effects to alter the observed glass transition temperature have been reported. Previously, this scheme has been used to observe molecular rotors in a short, mixed monolayer film[19] and artificial molecular rotors in three-dimensional arrays.[20,21]

RESULTS AND DISCUSSION

The interdigitated planar electrodes operate as a capacitor within which the dipolar molecules' temperature- and frequency-dependent motion alters the capacitance (directly related to the polarization) and the associated loss angle δ, which reflects the in-phase portion of the charging current (*i.e.*, the nonideality of the capacitor, measured by tan(δ)). In the experiment, both the dissipation factor tan(δ) as well as the capacitance are measured. The Debye form of the dissipation factor[16] is given as

$$\tan(\delta) = \frac{C}{C_0}\left(\frac{\omega\tau}{1+\omega^2\tau^2}\right) \quad (1)$$

where C_0 is the intrinsic capacitance of the bare electrodes (~1 pF), ω is the frequency of the applied electric field, and C is the capacitance due to the relaxing dipoles, with an average reorientation time of τ. Systematically varying the temperature from accessible cryogenic levels to well-above room temperature (10−400 K) alters τ over a wide range, whereas in our experiments, ω is restricted to 50 Hz and 20 kHz. Equation 1 has a maximum occurring at $\omega\tau = 1$; in addition, upon increasing to this temperature, the capacitance undergoes a step from C_0 to $C_0 + C$, where the thermally activated hopping of the dipoles (which governs τ) enables reorientation in response to the applied field of frequency, ω. This small step superimposed upon a capacitive (C_0) background that increases with temperature is generally more difficult to observe than the associated relaxation in tan(δ), which appears as a peak on a lower background. Thus we focus on tan(δ); however, each relaxation is also observed in the capacitance. The characteristic relaxation time τ can be described in several different formalisms. For local relaxations which are noncooperative, the Arrhenius form is appropriate:[16,22]

$$\frac{1}{\tau} = \omega_0 e^{\frac{-\Delta U}{kT}} \quad (2)$$

where ΔU is the energetic barrier associated with the motion of interest, k is Boltzmann's constant, T is the absolute temperature, and ω_0 is the attempt frequency; ω_0 is generally in the range of $10^{12}-10^{14}$ rad/s. Estimated from classical Eyring rate theory,[22,23] $\omega_0 \sim kT/h$, where h is Planck's constant. Starkweather[24−26] first associated artificially high attempt frequencies and correspondingly large activation energies with cooperative motion and argued that the free energy ΔG is the correct thermodynamic variable for the activation barrier

$$\Delta G = \Delta H - T\Delta S \quad (3)$$

where ΔH is the activation enthalpy and ΔS is the associated change in entropy, which will be zero for a local motion. Thus, for cooperative motion (where ΔS is significant), eq 3 results in a temperature independent term $e^{\Delta S/k}$, which multiplies the true ω_0 in eq 2 resulting in an artificially high observed attempt frequency. As an alternative to the Arrhenius form, for cooperative relaxations associated with a glass transition, the Vogel−Fulcher−Tammann (VFT) expression[27−29] is often used to define τ:

$$\frac{1}{\tau} = \omega_0 e^{\frac{-B}{(T-T_0)}} \quad (4)$$

where T_0 is a reference temperature and $\tau_0 = (\omega_0)^{-1}$ is customarily set to 10^{-14} s to reduce the number of free parameters.[30] Here the reference temperature T_0 represents a critical temperature, below which the free volume in the solid is approximately zero.[16] T_g, the glass transition temperature, can be obtained from this fit by extrapolating to $\tau = 100$ s.[31] One approach to classifying glass transitions is calculation of the fragility, quantified by the steepness index m, which is defined as[32]

$$m = \frac{d(\log(\tau))}{d(T_g/T)}_{T=T_g} \quad (5)$$

This treatment allows comparison of data from different systems; m values generally increase with increasing cooperativity. Because of the relatively narrow frequency range in our experiment, which enables the high sensitivity required to observe dynamics within monolayers, most Arrhenius plots ($\ln(1/\tau)$ *vs* $(1/T)$) display straight lines. By fitting with eq 2, the value of ω_0 can be used to determine if cooperative motion is present. For cooperative relaxations, a VFT fit can then be employed and subsequently extrapolated to estimate T_g and m.

Organosilane monolayer film samples of varying coverage, alkyl chain length, and structure were grown by either vapor- or solution-phase depositions onto the planar electrodes, as discussed in the Methods section. Sample coverage could be tuned from extremely dilute (submonolayer) to a complete monolayer by adjusting the length of time of the specific deposition.

The thickness of the sample films was inferred by measuring a silicon test wafer accompanying each sample, using a commercial null ellipsometer, where the organosilane films were considered to have approximately the same index of refraction as the native oxide layer of the silicon (~1.462[33]). Additional film characterization was made using water contact angle

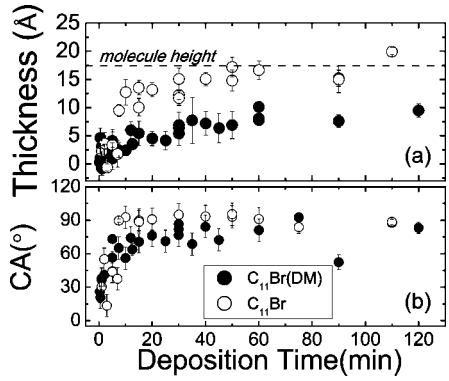

Figure 1. Comparison of vapor-deposited growth dynamics for monochlorosilane (C_{11}Br(DM) and trichlorosilane (C_{11}Br) molecules at 90 °C. (a) Ellipsometric measurements of film thickness *versus* time, where the labeled horizontal dashed line represents the height of near all-trans alkyl chain.[34] (b) Water contact angle (CA) measurements *versus* time.

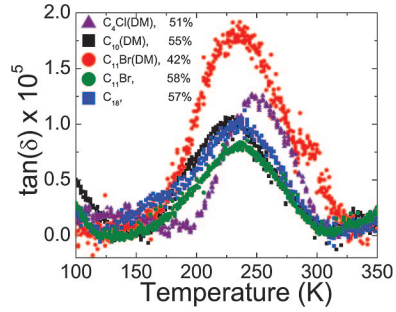

Figure 2. Varying the chain length: Films grown from molecules having 4−18 carbon atom chain lengths show a dielectric relaxation at ~235 K at 1 kHz measurement frequency: C_4Cl (purple triangles), C_{10}(DM) (black squares), C_{11}Br(DM) (red circles), C_{11}Br (green circles), and C_{18} (blue squares). The error on coverage is ±8%. Raw data points consisting of five measurements at each temperature are shown; resultant point error is typically smaller than the graphed data symbol's size.

measurements to determine the wettability of the coated surface and atomic force microscopy (AFM) measurements at ambient conditions, with image sizes of 5 × 5 μm or smaller, to reveal surface topography.

Figure 1 shows (a) ellipsometry and (b) contact angle measurements of vapor-deposition film growth curves for SAM samples using precursor monochlorosilane C_{11}Br(DM) and trichlorosilane (C_{11}Br) molecules, respectively. (Figure 6 in the Methods section schematically depicts the structure of these molecules.) Literature value for the all-trans configuration height of the attached molecule is indicated by the horizontal dashed line in Figure 1a. As expected, alkylsiloxane monolayers fabricated from monochlorosilanes have a maximum coverage of ~55% of the all-trans molecular height due to steric hindrance of the methyl groups, whereas SAMs created from trichlorosilanes can form a complete coverage monolayer, which results in the full molecular height as measured by ellipsometry.[35] AFM measurements show a surface variation of ±2 Å on the native silica oxide layer formed on a blank silicon test wafer; subsequent measurements on sample test wafers for vapor-deposited alkylsiloxane films grown to varying coverage resulted in similar variation, suggesting that vapor-deposited films grow homogeneously to form the SAM film. Both visual and quantitative analysis of AFM images reveal a homogeneous surface with no features. This growth pattern is in contrast to solution-phase depositions, which typically create SAMs by islanding mechanisms.[11]

Figure 2 shows tan(δ) *versus* temperature for film samples vapor-grown at 90 °C with ~60% coverage or less. Each sample has had a linear background subtracted (slope $<5 \times 10^{-8}$ tan(δ)/K) due to ionic conductivity. First, focusing on the result for C_{11}Br(DM) (red circles), a dielectrically active relaxation at ~235 K is evident. Aside from a well-known feature due to the fused silica substrate,[36] which appears at ~25 K (below the range displayed in Figure 2), no additional relaxations are observed over the temperature span of 10−400 K, which is equivalent to a 0.5 to 60 kJ/mol range of barriers (assuming Arrhenius dynamics and $\omega_0 = 10^{13}$ rad/s). The single sweep of a C_{11}Br(DM) film shown is representative of ~20 samples and ~57 individual experimental measurements at 1 kHz frequency on SAM samples at densities less than ~55% coverage measured over a period of 6 months. *C*, the capacitance due to the reorienting dipoles, can be determined by fitting a superposition of Debye peaks to the observed data, where *C* is proportional to the number of dipoles, the effective dipole moment, *p*, and a Curie factor, *p*/2*kT*, which reflects the interplay between random thermal energy and the interaction energy between the dipole and field (pE).[20] Such an amplitude analysis shows that the size of the dielectric relaxation is in good agreement with the estimated coverage from ellipsometry, giving an effective dipole moment of about 1.3 D, which falls between the estimates for an induced dipole near the siloxane linkage (~0.7 D) and the 1.8 D dipole expected for a bromomethyl group.

The dynamics of the 235 K relaxation as a function of temperature for the same C_{11}Br(DM) sample are shown (purple squares) in Figure 3. Two other samples of similar coverage are also plotted. Fitting the data with an Arrhenius form yields an artificially high attempt frequency $\ln(\omega_o) \sim 70$, revealing a cooperative motion. A VFT analysis yields a T_0 of 136 K. Both the VFT and Arrhenius plots are virtually linear over the relatively narrow frequency range measured. Extrapolating the VFT fits yields $T_g = 198 \pm 12$ K by averaging results from 12 samples on which multifrequency measurement temperature sweeps were taken. The estimated steepness index for this relaxation is 26 ± 7.

In order to most effectively elucidate the origin of this relaxation, low density samples grown from other alkylsilane molecules with differing chain lengths were measured, the results of which are also shown in Figure 2. Samples in this sequence possessed chain lengths

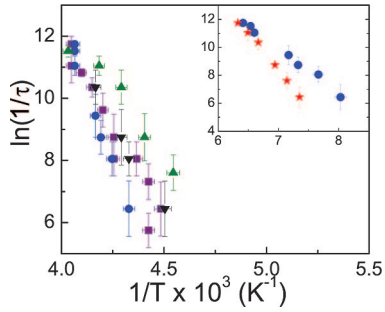

Figure 3. Arrhenius plot of ln(1/τ) *versus* (1/*T*). Data from the ~235 K interacting relaxation are plotted for C_{11}Br (DM) samples of 19% (upright green triangles), 42% (purple squares), and 49% (inverted black triangles) coverage and a 99% coverage C_{11}Br sample (blue circles). Inset: Corresponding ~150 K lower temperature relaxation from the 99% coverage C_{11}Br sample (blue circles) and a 55% C_{11}Br (DM) sample (red stars). The error in the coverage is ±8% for all samples.

varying from 4 to 18 carbon atoms; in addition, both mono- and trichlorosilanes were utilized in order to create films both having and lacking the ability to cross-link. Most films in this survey were generated at elevated temperatures from vapor phase, with the exception of C_4Cl(DM) as noted in the Methods section following. Finally, molecules with and without an explicit terminal dipole were also investigated. Previously, a broadband dielectric spectroscopy study of alkylsiloxane films, with and without explicit dipoles, grown on highly porous silica has been reported, concluding that the alkyl bonds closest to the silicon atom were polarized, resulting in a small net dipole and enabling the SAM to be dielectrically active.[18] We confirm this effect here by our observations shown in Figure 2, as both polar (explicit dipole) and nonpolar (no explicit dipole but an induced dipole near the siloxane linkage) films display a similar dielectric relaxation. In comparing signal size, C_{11}Br(DM), C_{11}Br, and C_{10}(DM) showed similar effective dipoles, which indicates that the dipole for the reorienting segments within the C_{11}Br samples may result from either an induced dipole near the surface (similar to that in the C_{10}(DM)) or the net effect of a permanent dipole (~1.8 D for a bromomethyl) counter-aligned with the induced dipole. C_{18} signal sizes were systematically smaller, at high coverage, than explicitly polar molecules; this may indicate a greater level of ordering, reducing the number of molecules free to reorient, or a smaller induced dipole in the C_{18} case. These observations with respect to amplitude are consistent with those previously reported.[18] In contrast to the longer chain films, samples with an alkyl chain less than four carbon atoms in length (TMS, C_1Cl(DM), C_3(DM), $C_3C{\equiv}N$(DM)) typically showed either no distinct relaxations, or relaxations significantly shifted toward lower temperature as compared with the relatively constant peak position of ~235 K observed in films composed of molecules with alkyl chains 4−18 carbon atoms in length. Relaxations in shorter films will be the subject of another detailed report. Although a careful examination of the data indicates subtle systematic changes in the dielectric spectra as a function of molecule type, dipole moment, coverage, preparation conditions, and thermal history, in this publication, we focus on the underlying *fundamental* relaxation common to all these *long* chain films. Considering measurement of all 22 samples of the various longer chain molecular species, $T_g = 200 \pm 11$ K and $m = 27 \pm 7$. We note that this collection of samples is heavily weighted toward the 11 carbon atom chain length due to the samples used.

Extensive research has been conducted on dynamics within polymers containing alkyl side chains, which shed light on the monolayer alkyl relaxations observed here. In particular, for alkyl side chain polymers, where the side chains are phase-separated, two distinct glass transitions have been reported.[17] One glass transition is consistent with the backbone relaxation and thus specific to the polymer type, whereas the other has been assigned to cooperative motion of the alkyl chains themselves, having only a weak dependence on backbone type. The authors identified this relaxation as polyethylene-like (PE-like) and observed a change in T_g of this α_{PE} as a function of chain length, due to the change in the size of the phase-segregated domains. The location of the α_{PE} relaxation was ~230−250 K in the 1 to 10 kHz range for a C_{10} chain, which is consistent with our observations. As chain length decreased, the domain size became smaller, which was associated with a shift in T_g toward lower temperatures (faster dynamics) and a decrease in fragility. At C_4, the relaxation had Arrhenius dynamics ($m = 16$). For C_{11}, m was approximately 37 and approached the PE value of $m \sim 50$ at chain lengths greater than 16 carbons. PE is a semicrystalline polymer, and thus its T_g varies with degree of crystallinity; however, the results from side chain polymers are consistent with PE values of $T_g = 190$ K for amorphous PE and $T_g = 260$ K for amorphous regions bound by crystalline material.[15]

These observations in polymers provide insight into the dynamics within the current system and match well with dielectric relaxation peaks observed with C_4−C_{18} chain lengths; in particular, the estimated T_g for our films is consistent with that of amorphous polyethylene, with a similar steepness index as observed for the polyethylene-like glass transition within side chain polymers. However, there are several distinct differences between our samples and the equivalent side chain polymers or neat polyethylene. In SAM samples, the substrate is correspondent to an extremely rigid backbone in a polymer system. Unlike a linear polymer, the substrate does not bend to allow phase segregation and the molecules are constrained to a two-dimensional sheet. Phase segregation may occur if small islands of molecules were formed; however, the size of these islands would have to be on the order <1

nm (a few molecules) in order to constrain the dynamics as seen in the polymer case. Thus phase segregation should play a reduced role. In limited studies, we found that *m* increased with density, as expected when molecule−molecule interactions increase in the low density regime. On the other hand, an alkylsiloxane SAM is also quite different than bulk PE because translational motion is strongly quenched from physical attachment to the surface. Thus, we do not expect to recover exactly the dynamics of either prototype system (alkyl side chain polymers or bulk PE). However, an analogous PE-like glass transition provides a reasonable hypothesis to explain these compelling dielectric observations.

As discussed above, most alkyl 2D SAMs reported in literature can be described as solid-like, having high density, usually close to the maximum packing density possible for alkyl chains of 18 Å^2,[37] and few gauche defects. These samples should be remarkably similar in nature to a single layer of a bulk alkane solid. Above the melting point of the alkane, densely packed samples become more liquid-like with the introduction of gauche defects at one or both ends of the chains. In order to create a liquid-like sample at room temperature, a lower density of molecules is necessary, allowing a significant number of gauche defects. Islanding, which depends on film deposition conditions and increases with chain length, must also be prevented. In fact, as discussed above, we specifically designed our fabrication technique toward formation of liquid-like monolayers, utilizing vapor-phase deposition at an elevated temperature, and silanes with bulky dimethyl groups, in order to prevent effective packing, so as to maximize the types of motional dynamics available to the alkyl chains. In order to display amorphous PE-like dynamics, the samples must be within the liquid-like regime, where chains are not ordered, at a distribution of tilt angles or in some manner lying down on the surface, and have a high density of gauche defects. In this environment, an ethyl group within the alkyl chain exists in a "soup" of other ethyl groups from neighboring chains, with little change in dynamics as a function of chain length. As discussed above, morphological studies support this assignment of our vapor-deposited films as liquid-like. In contrast, samples fabricated by room temperature solution-phase deposition of C_{11}Br exhibit island formation and display a shift in peak position toward lower temperatures and significant sharpening of the PE-like peak. (These expanded results will be discussed in a future publication.)

In order to further explore the relaxations within alkyl SAMs, we measured film samples with higher surface coverage. Whereas the maximum coverage of alkyl monolayers fabricated from monochlorosilane precursor molecules is limited to ~55%,[35] due to steric hindrance from the methyl groups, trichlorosilane molecules can obtain higher coverage and, potentially, a more ordered film. In general, for higher density coverage SAMs, including the highest density C_{11}Br(DM) obtained, a second relaxation at a lower temperature is observed. This relaxation was seen in C_{18}, C_{11}Br(DM), and C_{11}Br, at coverage greater than ~55%. Figure 4 shows a sequence of C_{11}Br SAMs grown from the vapor phase above room temperature. For the lowest coverage (~58%), only the 235 K relaxation is seen (see inset, Figure 4). As coverage increases (~99%), the 235 K peak gains in amplitude and a second relaxation appears at ~150 K. Escalating coverage further to the range of slight multilayering (average sample height 138% of an all-trans chain) results in no additional relaxations but increases the existing peak sizes. Figure 5 shows data for the 99% coverage sample at several frequencies to display shifting of the two peaks with frequency. These data are also expressed in the Arrhenius

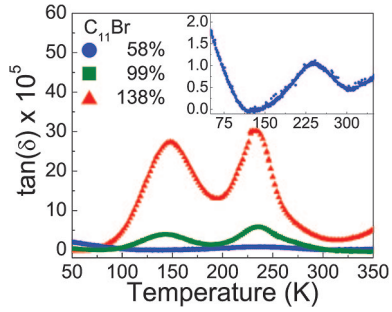

Figure 4. Varying the coverage for C_{11}Br SAMs: Dielectric relaxation at 1 kHz for films at submonolayer (58%, blue circles), monolayer (99%, green squares), and slight multilayer (138%, red triangles) coverage. All films display a peak at ~235 K; as coverage increases, a second relaxation at ~150 K also appears. Inset: an expanded view of the 58% C_{11}Br SAM showing only the ~235 K relaxation. Raw data points consisting of five measurements at each temperature are shown; resultant point error is typically smaller than the graphed data symbol's size. The error in the coverage is ±8% for all samples.

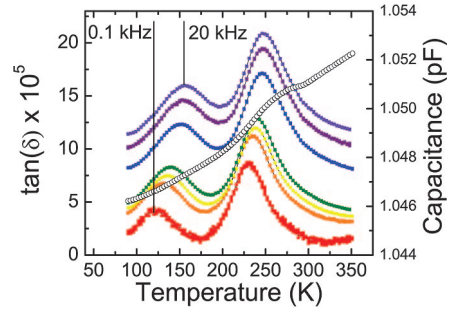

Figure 5. Dielectric spectroscopy of a full coverage (99%) C_{11}Br SAM. Loss (left axis, tan(δ)) measured with applied frequencies of 0.1, 0.5, 1, 2, 10, 16, and 20 kHz as a function of sample temperature. Representative vertical lines at 0.1 and 20 kHz are drawn at each lower temperature maximum, respectively, to aid the eye in demonstrating the dispersive nature of the relaxation. Raw data points consisting of five measurements at each temperature are shown; resultant point error is typically smaller than the graphed data symbol's size. The corresponding stepwise change is shown in the capacitance for 1 kHz (right axis (open circles)).

form in Figure 3. Unlike the interacting dynamics of the higher temperature relaxation, the ~150 K relaxation displayed Arrhenius dynamics and a barrier E_b = 29.7 ± 3.8 kJ/mol, an average value resulting from eight samples.

We compare our results in this coverage regime to a recent report of broadband dielectric relaxation spectroscopy on siloxane SAMs grown on porous glass powders.[18] In that work, samples of C_{18} fabricated by solution phase at relative coverage of 51−80% display a relaxation with effective activation energy of ~25 kJ/mol. The authors connect this relaxation with the known γ processes in PE, such as trans-gauche reorientations and the rotation of short chain segments. Equivalent localized relaxations are also present in alkyl side chain polymers, with side chains greater than four carbon atoms in length, as was first reported in the early 1970s.[38] In particular, the γ relaxations in alkyl side chain polymers follow Arrhenius dynamics and have barriers that range from 23 to 37 kJ/mol[39−41] consistent with our observations and those previously published.[18]

CONCLUSIONS

In summary, we demonstrate the ability to observe dynamics within dilute chemisorbed monolayers *via* a novel dielectric spectroscopy approach with sufficient sensitivity to utilize the induced dipole in a functionalized alkyl chain as a marker of motion. Over a range of coverage from ~10% to slight multilayers, for molecules with chain lengths of 4−18 carbon atoms, and in the presence and absence of cross-linking, we observe a cooperative relaxation, which has the characteristics of a polyethylene-like glass transition. Samples for these studies were fabricated from vapor phase at elevated temperature in order to deliberately generate liquid-like, disordered films. As coverage increases, a second, local relaxation, with similar dynamics and barrier to a γ relaxation in polyethylene, is also observed. This relaxation may result from a reduction in the number of gauche defects as the packing density increases and chains are forced to straighten, providing four-carbon segments that are primarily in a trans configuration.

METHODS

Organosilane monolayer film samples of varying coverage, alkyl chain length, and structure were grown by either vapor- or solution-phase depositions onto the planar electrodes. Gold interdigitated electrodes on fused silica substrates, with 26 1 mm long finger pairs with equal spacing and width of 10 μm, were fabricated using standard UV lithography. Alkyldimethylchlorosilanes with one reactive group for attachment to the surface and chain lengths of 4 to 11 carbon atoms are discussed in this paper.

In particular, chlorobutyldimethylchlorosilane (C_4Cl (DM)), *n*-decyldimethylchlorosilane (C_{10}(DM)), and 11-bromoundecyldimethylchlorosilane (C_{11}Br(DM)) were utilized. Alkyltrichlorosilanes, which have three reactive groups and thus can form cross-linked films, with 11, 11-bromoundecyltrichlorosilane (C_{11}Br) or 18, octadecyltrichlorosilane (C_{18}), carbon atom chains were also utilized. Shorter chain molecules (trimethylchlorosilane TMS, chloromethyldimethylchlorosilane C_1Cl(DM), *n*-propyldimethylchlorosilane C_3(DM), and 3-cyanopropyldimethylchlorosilane $C_3C{\equiv}N$(DM)) were also measured as controls and will be discussed in more detail in a future report. Molecules were purchased from Sigma Aldrich (C_{18}) or Gelest and used without further purification. Prior to film growth, the sample planar electrode and a silicon test wafer were twice cleaned in a UV surface decontaminator for 30 min (exposed to oxygen for the first 10 min), rinsed with deionized water, and dried with nitrogen. Vapor-deposited films of C_{10}(DM), C_{11}Br(DM), C_{11}Br, and C_{18} were obtained by uniformly heating a covered, presilanated, Pyrex deposition vessel containing the electrode and wafer to 90 °C for 30 min to reach thermal equilibrium. Twenty microliters of molecules was then added to the vessel, and the film growth proceeded for a specified time interval. C_4Cl(DM) vapor depositions followed the same procedure but were performed at room temperature in a nitrogen-purged dry box (<2% relative humidity). Monolayer samples of C_{11}Br were also fabricated in solution phase by immersing the wafer and electrode in 20 mL of toluene at ambient temperature in the dry box, then adding 20 μL of molecules. Sample coverage could be tuned from extremely dilute (submonolayer) to a complete monolayer by adjusting the length of time of the specific deposition. After film growth, the samples and test wafers were rinsed with methanol or toluene, sonicated in methanol or toluene, rinsed again with purified water, and blown dry with nitrogen gas. We note that subsequent film thickness measurements showed that the initial alcohol rinse is sufficient to remove the majority of physisorbed molecules from the surface; the sonication and additional rinsing step did not reduce measured film thickness.

The thickness of the sample films was inferred by measuring the appropriate silicon test wafer accompanying each sample, using a commercial null ellipsometer with a 70° incident angle. The organosilane films were considered to have approximately the same index of refraction as the native oxide layer of the silicon (~1.462[33]). Typically, six data points were taken at different spatial locations on the surface of the silicon test wafer before and after the deposition; the averaged difference between the ellipsometry measurements determined the genuine film growth. The system displays an intrinsic overall resolution of

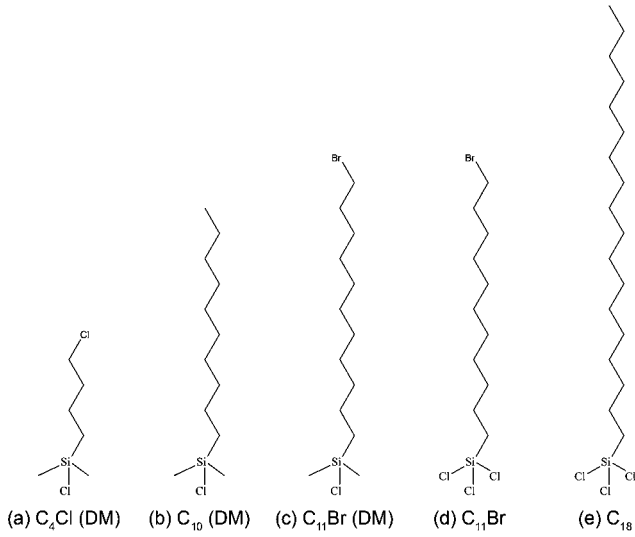

Figure 6. Schematic depiction of the molecules used to form the monolayers. (a) Chlorobutyldimethylchlorosilane (C_4Cl (DM)), (b) *n*-decyldimethylchlorosilane (C_{10}(DM)), (c) 11-bromoundecyldimethylchlorosilane (C_{11}Br(DM)), (d) 11-bromoundecyltrichlorosilane (C_{11}Br), and (e) octadecyltrichlorosilane (C_{18}).

±1Å, which corresponds to a minimum coverage estimate error of ±5% for a ~20 Å tall molecular film. In addition to ellipsometry, water contact angle measurements determined the wettability of the coated surface, and atomic force microscopy (AFM) measurements at ambient conditions, with image sizes of 5 × 5 μm or smaller, revealed surface topography.

Temperature-dependent capacitance and dielectric loss spectra were measured in vacuum in two independent systems: a cryogenic probe station and an ultrahigh vacuum chamber installed with a commercial custom-designed cold head. The prober system (cold head) enables temperature scans from 80 to 380 K (10 to 400 K) and achieves an oil-free vacuum level of $\sim 10^{-6}$ (10^{-8}) Torr when the sample is at ambient temperature. The use of dual measurement systems allows cross-checking for systematic errors and elimination of any effects due to contacts (made by micromanipulator probes or permanent bonded contacts, respectively) or vacuum levels. Dielectric relaxation spectra in each of the systems were measured at multiple user-selected distinct sine-wave frequencies between 50 Hz and 20 kHz with an amplitude of 5−15 V_{rms} using single and multifrequency precision Andeen−Hagerling capacitance bridges. A typical data sweep makes five individual measurements per frequency at each temperature, with 5 s settling time between measurements. Typical temperature steps were 2−3 K with 3−5 min equilibration time between temperatures.

Acknowledgment. We gratefully acknowledge funding in the form of NSF Grant 04-03871, use of force microscopy facilities in the Robert Nemanich and Jack Rowe research groups, and use of dry solvents from the Chris Gorman research group. The authors would also like to thank A. Hewitt for contributions to the contact angle and siloxane film growth curve measurements.

REFERENCES AND NOTES

1. Fendler, J. H. Chemical Self-Assembly for Electronic Applications. *Chem. Mater.* **2001**, *13*, 3196–3210.
2. Smith, R. K.; Lewis, P. A.; Weiss, P. S. Patterning Self-Assembled Monolayers. *Prog. Surf. Sci.* **2004**, *75*, 1–68.
3. Li, X. M.; Huskens, J.; Reinhoudt, D. N. Reactive Self-Assembled Monolayers on Flat and Nanoparticle Surfaces, and Their Application in Soft and Scanning Probe Lithographic Nanofabrication Technologies. *J. Mater. Chem.* **2004**, *14*, 2954–2971.
4. Katsonis, N.; Lubomska, M.; Pollard, M. M.; Feringa, B. L.; Rudolf, P. Synthetic Light-Activated Molecular Switches and Motors on Surfaces. *Prog. Surf. Sci.* **2007**, *82*, 407–434.
5. Chaki, N. K.; Vijayamohanan, K. Self-Assembled Monolayers as a Tunable Platform for Biosensor Applications. *Biosens. Bioelectron.* **2002**, *17*, 1–12.
6. Wise, S. A.; Sander, L. C.; May, W. E. Determination of Polycyclic Aromatic-Hydrocarbons by Liquid-Chromatography. *J. Chromatogr.* **1993**, *642*, 329–349.
7. Saito, Y.; Ohta, H.; Jinno, K. Design and Characterization of Novel Stationary Phases Based on Retention Behavior Studies with Various Aromatic Compounds. *J. Sep. Sci.* **2003**, *26*, 225–241.
8. Sander, L. C.; Wise, S. A. Shape Selectivity in Reversed-Phase Liquid-Chromatography for the Separation of Planar and Nonplanar Solutes. *J. Chromatogr., A* **1993**, *656*, 335–351.
9. Hostetler, M. J.; Murray, R. W. Colloids and Self-Assembled Monolayers. *Curr. Opin. Colloid Interface Sci.* **1997**, *2*, 42–50.
10. Badia, A.; Lennox, R. B.; Reven, L. A Dynamic View of Self-Assembled Monolayers. *Acc. Chem. Res.* **2000**, *33*, 475–481.
11. Schreiber, F. Structure and Growth of Self-Assembling Monolayers. *Prog. Surf. Sci.* **2000**, *65*, 151–256.
12. Vericat, C.; Vela, M. E.; Salvarezza, R. C. Self-Assembled Monolayers of Alkanethiols on Au(111): Surface Structures, Defects and Dynamics. *Phys. Chem. Chem. Phys.* **2005**, *7*, 3258–3268.
13. Kottas, G. S.; Clarke, L. I.; Horinek, D.; Michl, J. Artificial Molecular Rotors. *Chem. Rev.* **2005**, *105*, 1281–1376.
14. Maroncelli, M.; Qi, S. P.; Strauss, H. L.; Snyder, R. G. Nonplanar Conformers and the Phase-Behavior of Solid *n*-Alkanes. *J. Am. Chem. Soc.* **1982**, *104*, 6237–6247.
15. Lam, R.; Geil, P. H. T_g of Amorphous Linear Polyethylene—Torsion Braid Analysis. *Polym. Bull.* **1978**, *1*, 127–131.
16. McCrum, N. G.; Read, B. E.; Williams, G. *Anelastic and Dielectric Effects in Polymeric Solids*; Dover: New York, 1991.
17. Beiner, M.; Huth, H. Nanophase Separation and Hindered Glass Transition in Side-Chain Polymers. *Nat. Mater.* **2003**, *2*, 595–599.
18. Zhang, Q.; Zhang, Q.; Archer, L. A. Molecular Relaxation Dynamics of Self-Assembled Monolayers. *J. Phys. Chem. B* **2006**, *110*, 4924–4928.
19. Clarke, L. I.; Horinek, D.; Kottas, G. S.; Varaksa, N.; Magnera, T. F.; Hinderer, T. P.; Horansky, R. D.; Michl, J.; Price, J. C. The Dielectric Response of Chloromethylsilyl and Dichloromethylsilyl Dipolar Rotors on Fused Silica Surfaces. *Nanotechnology* **2002**, *13*, 533–540.
20. Horansky, R. D.; Clarke, L. I.; Price, J. C.; Khuong, T. A. V.; Jarowski, P. D.; Garcia-Garibay, M. A. Dielectric Response of a Dipolar Molecular Rotor Crystal. *Phys. Rev. B* **2005**, *72*, 14302-1–14302-5.
21. Horansky, R. D.; Clarke, L. I.; Winston, E. B.; Price, J. C. Dipolar Rotor−Rotor Interactions in a Difluorobenzene Molecular Rotor Crystal. *Phys. Rev. B* **2006**, *74*, 54306-1–54306-12.
22. Mano, J. F.; Lanceros-Mendez, S. Simple *versus* Cooperative Relaxations in Complex Correlated Systems. *J. Appl. Phys.* **2001**, *89*, 1844–1849.
23. Cagle, F. W., Jr.; Eyring, H. An Application of the Absolute Rate Theory to Phase Changes in Solids. *J. Phys. Chem.* **1953**, *57*, 942–946.
24. Starkweather, H. W. Simple and Complex Relaxations. *Macromolecules* **1981**, *14*, 1277–1281.
25. Starkweather, H. W. Noncooperative Relaxations. *Macromolecules* **1988**, *21*, 1798–1802.
26. David, L.; Etienne, S. Molecular Mobility in Para-Substituted Polyaryls. 1. Sub-T(G) Relaxation Phenomena in Poly(aryl ether ether ketone). *Macromolecules* **1992**, *25*, 4302–4308.
27. Fulcher, G. S. Analysis of Recent Measurements of the Viscosity of Glasses. *J. Am. Ceram. Soc.* **1925**, *8*, 339–355.
28. Tammann, G.; Hesse, W. The Dependancy of Viscosity on Temperature in Hypothermic Liquids. *Z. Anorg. Allg. Chem.* **1926**, *156*, 245–257.
29. Vogel, H. The Temperature Dependence Law of the Viscosity of Fluids. *Phys. Z* **1921**, *22*, 645–646.
30. Santangelo, P. G.; Roland, C. M. Molecular Weight Dependence of Fragility in Polystyrene. *Macromolecules* **1998**, *31*, 4581–4585.
31. Angell, C. A. Formation of Glasses from Liquids and Biopolymers. *Science* **1995**, *267*, 1924–1935.
32. Bohmer, R.; Ngai, K. L.; Angell, C. A.; Plazek, D. J. Nonexponential Relaxations in Strong and Fragile Glass Formers. *J. Chem. Phys.* **1993**, *99*, 4201–4209.
33. Ulman, A. *An Introduction to Ultrathin Organic Films: from Langmuir−Blodgett to Self-Assembly*; Academic Press: Boston, 1991; p 442.
34. Wasserman, S. Structure and Reactivity of Alkylsiloxane Monolayers Formed by Reaction of Alkyltrichlorosilanes on Silicon Substrates. *Langmuir* **1989**, *5*, 1074–1087.
35. Genzer, J.; Efimenko, K.; Fischer, D. A. Molecular Orientation and Grafting Density in Semifluorinated Self-Assembled Monolayers of Mono-, Di-, and Trichloro Silanes on Silica Substrates. *Langmuir* **2002**, *18*, 9307–9311.
36. Ozaki, T.; Ogasawara, T.; Kosugi, T.; Kamada, T. Dielectric Dispersion of SiO_2 Glass at Low Temperatures. *Phys. B* **1999**, *263*, 333–335.
37. Pomerantz, M.; Segmüller, A.; Netzer, L.; Sagiv, J. Coverage of Si Substrates by Self-Assembling Monolayers and Multilayers as Measured by IR, Wettability and X-ray Diffraction. *Thin Solid Films* **1985**, *132*, 153–162.
38. Shimizu, K.; Yano, O.; Wada, Y. Dielectric Study of Low-Temperature Relaxations in Poly(Isobutyl Methacrylate), Poly(*n*-Butyl Methacrylate), Poly(Isopropyl Methacrylate),

and Poly(4-Methylpentene-1). *J. Polym. Sci., Part B: Polym. Phys.* **1975**, *13*, 1959–1974.
39. Genix, A. C.; Laupretre, F. Subglass and Glass Transitions of Poly(Di-*n*-Alkylitaconate)s with Various Side-Chain Lengths: Dielectric Relaxation Investigation. *Macromolecules* **2005**, *38*, 2786–2794.
40. Grimau, M.; Laredo, E.; Sanchez, F.; Lopez-Carrasquero, F.; Baez, M. E.; Bello, A. Molecular Dynamics in Nanophase-Separated Comb-Like Poly(Alpha-*n*-Alkyl Beta-L-Aspartate)s. *Eur. Phys. J. E* **2004**, *15*, 383–393.
41. Sanchis, M. J.; Diaz-Calleja, R.; Pelissou, O.; Gargallo, L.; Radic, D. Dynamic Mechanical and Dielectric Relaxations in Poly(Di-*n*-Chloroalkylitaconates). *Polymer* **2004**, *45*, 1845–1855.